An Adaptive Soft-Sensor for Non-Destructive Cement-Based Material Testing, through the Use of RBF Networks

Alex Alexandridis, Dimos Triantis, Eva Chondrodima, Charalampos Stergiopoulos, George Hloupis, Ilias Stavrakas, Konstantinos Ninos
Department of Electronics
Technological Educational Institute of Athens
Athens, Greece
alexx@teiath.gr

***Abstract*—This paper presents the development of a soft-sensor receiving as inputs Pressure Stimulated Current (PSC) characteristics in order to predict a critical mechanical property of cement-based materials, in a non-destructive manner. The soft-sensor is based on a Radial Basis Function (RBF) network that starts with an empty hidden layer and evolves its structure and synaptic weights as new data become available. Results have shown that the proposed approach can be used successfully to evolve a predictive tool based on input-output data, whereas it is superior compared to other adaptive modeling techniques.**

Keywords- Adaptive Soft-Sensors; Radial Basis Function; Fuzzy Means; Non-Destructive Testing; Pressure Stimulated Currents

I. INTRODUCTION

Soft-Sensors are virtual sensors, with the ability to estimate the values of physical quantities, without actually measuring them. Soft-sensors usually employ input variables that are associated with the physical quantity to be estimated, but can be measured with less effort and/or cost.

Based on the approach used for producing the correlation, soft-sensors can be categorized as model-driven or data-driven [1]. Model-driven soft-sensors rely on First Principle models in order to describe the mechanisms that correlate the measured variables with the variable to be estimated. The development of such models can be rather cumbersome and time-consuming, as quite often the physicochemical phenomena that lie in the background are poorly understood. Furthermore, such models are process-specific, so their applicability is rather limited. Data-driven sensors on the other hand, do not require any first principle-based description of the process, but are based solely on historical data derived from it. The recorded data are usually correlated using computational techniques including neural networks, fuzzy logic, multivariate statistical methods, etc.

Neural networks (NNs) are a set of powerful mathematical tools [2] that simulate the way that the human brain deals with information and the procedure of learning. NNs have the ability to identify and learn highly complex and nonlinear relationships by employing a black-box approach, i.e. without requiring any *a priori* knowledge about the process, but based on input- output data only. This ability has made neural networks very popular in the development of data-driven soft-sensors. A soft computing approach based on neural networks has been employed in [3], in order to perform fault detection in gas turbine engines. In [4], the authors present a number of strategies for improving the generalization capabilities of neural network–based soft-sensors when small data sets are available. Recently [5], a predictive tool for non-destructive testing of cement-based materials has been proposed, based on Radial Basis Function (RBF) neural networks

Though such tools have been proven able to provide accurate predictions in static environments, they cannot take into account data retrieved from new experiments. To this end, there is an increasing interest in the development of adaptive soft-sensors, i.e. soft-sensors based on models with the ability to adapt their parameters online to new information coming from the system under identification [6-8]. In [1], the authors present an adaptive soft-sensor which can be deployed in real-life environments. In [9], an adaptive soft-sensor based on neural networks is presented. The authors report a successful application of the soft-sensor to an advanced control system

In this work, we present an adaptive soft-sensor for testing cement-based materials in a non-destructive manner. The soft-sensor is based on information contained in weak electrical signals appearing within materials subjected to mechanical stress, in order to evolve RBF networks with the ability to predict the compressive strength of the specimens. Using an adaptive RBF network learning scheme, the soft-sensor can change its parameters in order to take into account new data, thus accumulating information about the system's behavior.

The rest of this paper is organized as follows: In the next section, we present the soft-sensor experimental arrangement, giving a brief overview of the Pressure Stimulated Currents (PSC) technique and describing the PSC characteristics used as inputs to the soft-sensor. In section 3, we outline the adaptive RBF network training methodology, used for evolving the RBF model lying in the heart of the soft-sensor. Section 4 illustrates the adaptive soft-sensor development, and provides results from its application on experimental data. The paper concludes by outlining the advantages of the proposed approach.

978-1-4673-1727-6/12/$31.00 ©2013 IEEE

II. Soft-Sensor Experimental Arrangement

A. The PSC Technique

The PSC technique is based on measuring the weak electrical signals that are generated within a specimen when the latter is subjected to compressive mechanical stress [10-13]. Studies have shown that even at low compressive stress levels, several characteristics of the recorded electrical signals contain information related to the ultimate compressive strength of the specimen (i.e. the compressive strength level associated with specimen failure). Compressive strength is a critical mechanical property of concrete and other construction materials, and is commonly used as a performance indicator for structural design.

This section describes briefly the PSC methodology and the relative experimental procedure in order to implement the soft-sensor. For a more detailed description of the experimental arrangement, together with the preparation of the specimens and their characteristics, the interested reader is referred to previous works [5, 10].

The particular experimental procedure, known as the High Rate Step Stress (HRSS) technique, is described by an abrupt, almost linear, increase of the mechanical stress at a high rate, aiming to simulate a step change. The temporal description $\sigma(t)$ of stress during this procedure is described as:

$$\sigma(t)=\begin{cases}\sigma_L=\text{constant} & \text{for} \quad t<t_L\\ \sigma_L+b(t-t_L) & \text{for} \quad t_L\le t\le t_H\\ \sigma_H=\sigma_L+\Delta\sigma & \text{for} \quad t>t_H\end{cases} \tag{1}$$

where σ_L is the initial constant uniaxial stress applied on the specimen, t_L and t_H are the time instants where the change begins and ends respectively, σ_H is the higher stress level and $b=\Delta\sigma/\Delta t$ is the rate of increase of the mechanical stress.

The emitted PSC signal and the mechanical stress are recorded by a sensitive programmable electrometer and a pair of gold plated electrodes respectively, both attached on the specimen body. The recorded signals are transferred through a General Purpose Interface Bus (GPIB) and an Analogue to Digital Converter on a PC. The experimental arrangement is shown schematically in Fig. 1.

B. PSC characteristics to be used as inputs to the soft-sensor

The recorded PSC signals should be analyzed to extract those characteristics that contain the maximum amount of information, in order to be used as inputs to the soft-sensor.

Figs. 2a and b depict a typical PSC signal recording while applying the HRSS technique, together with the temporal variation of the mechanical stress. This experiment started with a low stress level σ_L equal to 12.1MPa which increased abruptly within 3*s* approximately, to a high stress level σ_H of 22.5MPa. The applied stress remained on the specimen at the high level for a time period of approximately 200s and then an additional stress increase was attempted in order to determine the ultimate compressive stress strength σ_f, during which the specimen failed at a stress value of 33.5MPa.

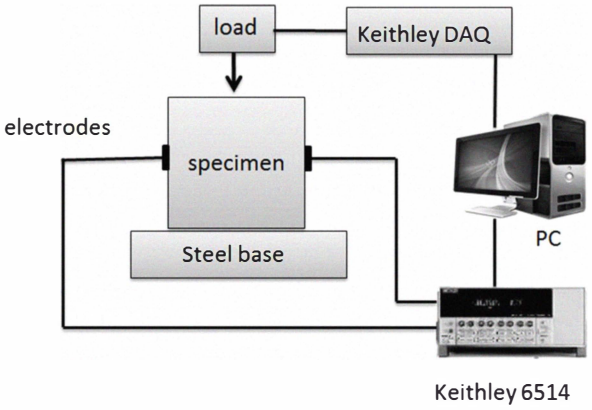

Figure 1. Experimental arrangement for measuring PSC signals [5]

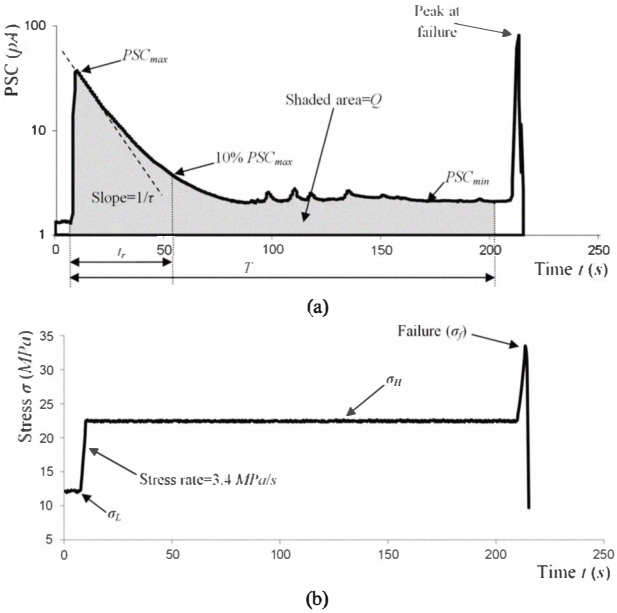

Figure 2. A typical PSC signal recording depicting: (a) the various PSC characteristics to be used as input to the soft-sensor and (b) the temporal variation of the mechanical stress [5]

When the σ_H level is far from the fracture limit, the application of the abrupt stress step is immediately followed by a PSC spike (PSC_{max}), which is an important characteristic of the PSC response. Following the stress settlement at the levels of σ_H, the PSC signal begins gradually decreasing (see Fig. 2a), obeying the following exponential decrease law:

$$PSC(t-t_0)=PSC_{\max}\cdot\exp\left(-\frac{t-t_0}{\tau}\right) \tag{2}$$

where t_0 is the moment that PSC has reached its maximum value (which practically corresponds to time t_H when the step-stress has been completed), and τ is a time constant which is characteristic of the time needed for the restoration of the PSC signal. Consequently, the PSC signal reaches a low background level PSC_{min}, and then exhibits small fluctuations around this level. There are two additional characteristic parameters of a PSC signal that present interest: The first one is the total released electric charge Q during each experiment according to the equation:

$$Q = \int_{t_H}^{t_H+T} PSC(t)dt \tag{3}$$

Another parameter associated with the fast and slow restoration of a PSC signal is the time duration t_r needed for the PSC signal to reach the critical value of 10% of its maximum value PSC_{max}.

As soon as the second stress increase takes place, a second PSC signal spike occurs, followed by the specimen failure.

III. The Adaptive Fuzzy Means Algorithm for Training RBF Networks

A. RBF networks and offline training

RBF networks form a special neural network architecture that consists of three layers (Fig. 3).

The RBF network training procedure corresponds to determining the hidden node basis function parameters and the output-layer weights. Standard approaches in offline RBF network training, decompose this problem in two steps: In the first step, the hidden layer basis function parameters are obtained using an unsupervised clustering technique, like the *k*-means algorithm [14]. The second step involves determination of the output-layer weights by linear least squares regression.

B. Adaptive RBF network training

An adaptive version of the fuzzy means algorithm has been introduced [15], allowing the RBF network to adapt its parameters online to new data received from the system under identification. The adaptive version does not need an initial neural network model. It starts with zero hidden nodes and progressively builds the model as new data become available. Obviously, the predictions of the model are not very successful in the first steps, but as soon as more data are fed into the network, the prediction ability of the network is gradually improved.

The adaptive technique which will be described briefly in this section, relies on a fuzzy partition of the input space, as implemented by the standard fuzzy means algorithm. The method considers all the centers of the fuzzy subspaces as

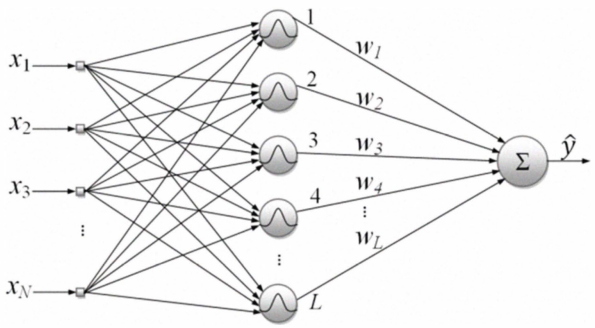

Figure 3. Typical structure of an RBF network

candidates for locating the hidden nodes of the network. However, among all the candidate centers, the algorithm dynamically identifies and selects only the subset of fuzzy subspaces that are close to the input examples. At each time instant the number of selected fuzzy subspaces is equal to the number of nodes in the hidden layer and the centers of the selected subspaces coincide with the centers of the hidden nodes. Therefore, at any time point a complete RBF model is available, which is first used for predicting the future behavior of the output variables and then is updated based on the proposed algorithm.

The adaptive fuzzy means algorithm evolves the RBF network based on two levels of adaptation, namely:

a) Adaptation of the connection weights between the hidden layer and the output layer.

b) Adaptation of the structure of the hidden layer based on a fuzzy partition of the input space.

An overview of the algorithm is given in Fig. 4.

As far as the first level of adaptation is concerned, the connection weights **w** of the hidden layer are updated using the RLS algorithm, according to the following equations:

$$\begin{aligned} \mathbf{w}(k) &= \mathbf{w}(k-1) + \mathbf{q}(k)\left(y(k) - \mathbf{z}^T(k)\mathbf{w}(k-1)\right) \\ \mathbf{q}(k) &= \mathbf{P}(k-1)\mathbf{z}(k)\left(\lambda + \mathbf{z}^T(k)\mathbf{P}(k-1)\mathbf{z}(k)\right)^{-1} \\ \mathbf{P}(k) &= \left(\mathbf{I} - \mathbf{q}(k)\mathbf{z}^T(k)\right)\mathbf{P}(k-1)/\lambda \end{aligned} \tag{4}$$

where k stands for the current sample number, **z** are the responses of the hidden layer nodes, **P** is the inverse of the covariance matrix, and λ is the forgetting factor. Applying the forgetting factor implies that a data point that is n times old, will be weighted by λ^n

However, due to the local approximation approach of RBF networks, this type of adaptation may not be adequate when a new data point arrives which is not sufficiently covered by the existing centers. In order to address this situation, the algorithm introduces the second level of adaptation, where new hidden

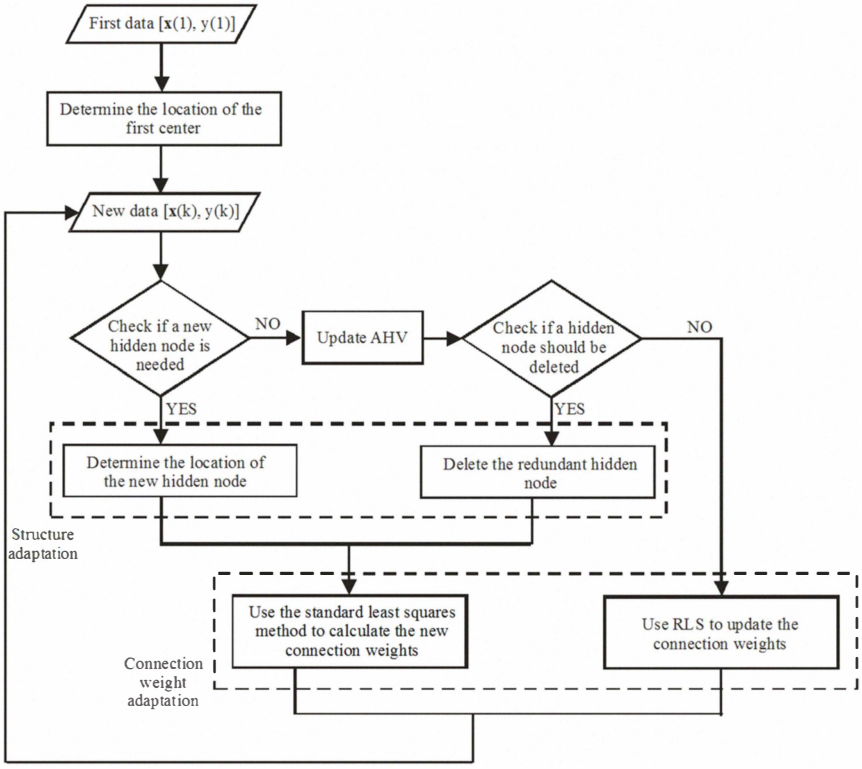

Figure 4. Overview of the adaptive fuzzy means algorithm

nodes are added in order to describe data points that lie outside of the area covered by existing centers. As the continuous addition of hidden nodes could lead to large network configurations and increased computational complexity, the algorithm also provides suitable means for deleting hidden nodes when they become redundant.

As soon as the first input example arrives from the system, the algorithm determines the fuzzy subspace that is closer to that data point in the relative Euclidean distance sense [16]. The center of this subspace becomes the center of the first hidden node and the respective fuzzy subspace initializes the list of the selected subspaces. As soon as the first hidden node is determined, the algorithm initiates two dynamic matrices, which are used to store important information. These are the Center Location Matrix (CLM) **G** and the Activation History Vector (AHV) **h**. The CLM contains at each time instant the centers of the hidden layer nodes and its dimension is LxN where L is the number of the selected RBF centers and N is the dimensionality of the input space. The structure of CLM is depicted in Fig. 5. The size of the AHV is equal to the number of the selected RBF centers L and contains the last time instant that an input example was assigned to each fuzzy subspace.

When a new input example becomes available, the algorithm first checks whether the input vector can be assigned to an already selected fuzzy subspace. If the answer is negative, a new node should be added to the hidden layer. This is achieved by selecting the fuzzy subspace which is closer to the input vector in the Euclidean relative distance sense and locating the center of the new hidden node, at the center of the selected subspace. In this case, the new center is added to the CLM and the information in the AHV is updated

If the algorithm decides that no new hidden node is needed, it checks whether an existing hidden node has not been assigned recently to an input vector. If this is true, the hidden node is deleted and the respective fuzzy subspace is removed from the list of selected subspaces. In this way, the algorithm manages to sustain a number of hidden nodes that is sufficient enough to describe the system, but at the same time the structure of the network is kept within a reasonable size.

In case a center is added or deleted, the connection weights between the hidden layer and the output layer need to be

$$\mathbf{G} = \begin{bmatrix} G_{11} & G_{12} & \cdots & G_{1N} \\ G_{21} & G_{22} & \cdots & G_{2N} \\ \vdots & \vdots & \ddots & \vdots \\ G_{i1} & G_{i2} & \cdots & G_{iN} \\ \vdots & \vdots & \ddots & \vdots \\ G_{L1} & G_{L2} & \cdots & G_{LN} \end{bmatrix}$$

Coordinates for the i*th* center

Figure 5. Structure of the dynamically changing Center Location Matrix

recalculated. This is achieved by using a moving time window, where a number of past input-output data are stored. The connection weights are obtained by regressing the outputs of the hidden layer (formulated after the addition or deletion of a node) on the real outputs of the system.

If the structure of the hidden layer remains unaltered, the method does not change the locations of the hidden node centers and updates only the connection weights between the hidden layer and the output layer using the RLS with exponential forgetting algorithm.

More details regarding the online RBF training methodology can be found in the original publication [15].

IV. Adaptive Soft-Sensor Development and Testing

A. Adaptive soft-sensor development

The basis for the development of the adaptive soft-sensor is a neural network model, correlating the ultimate compressive strength of specimens σ_f, with the five input variables corresponding to the critical PSC characteristics presented in section II, and the higher stress level σ_H. The neural network predictions are given by:

$$\hat{\sigma}_f = RBF\left(PSC_{max}, PSC_{min}, \tau, t_r, Q, \sigma_H\right) \quad (5)$$

where *RBF* stands for the nonlinear function implemented by the RBF network.

The RBF network is initialized with an empty hidden layer. As soon as the first training example becomes available, the first hidden node is added and the soft-sensor is ready to provide predictions. Following every experiment, the soft-sensor adaptation mechanism is presented with a new input-output data point. Based on the adaptive fuzzy means algorithm, the structure and the synaptic weights of the RBF network are evolved in order to describe the information contained in the new examples. Meanwhile the soft-sensor is available for providing predictions based on extracted PSC characteristics from specimens under non-destructive testing. The soft-sensor operation is visually depicted in Fig. 6.

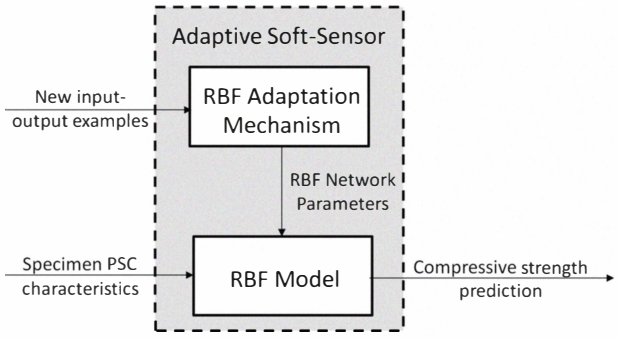

Figure 6. Adaptive soft-sensor operational scheme

B. Results and discussion

In order to test the proposed adaptive soft-sensor, a series of lab experiments was set up to obtain the necessary input-output data for training. Each available specimen was subjected to a low compressive stress, and the PSC emissions were recorded and analyzed in order to extract the necessary characteristics. The PSC characteristics were then used as inputs to the adaptive soft-sensor, triggering a prediction for the ultimate compressive strength of the specimen. After obtaining the prediction, the compressive stress was increased until the specimen failed. The real value for the ultimate compressive strength was recorded and then the soft-sensor was allowed to adapt itself to the newly available input-output example. For the first three specimens, the prediction stage was omitted, since the RBF network was too early in its development to give meaningful predictions.

For comparison purposes, an additional adaptive model based on Multi-Layer Perceptron (MLP) networks trained with an online back-propagation algorithm [2] was also tested. Results from the application of the two adaptive models are summarized in Figs 7-9, depicting the ultimate compressive strength prediction for each specimen (together with the measured values), the evolution of the RBF hidden node centers, and the Absolute Relative Error% (ARE%), respectively. As it can be seen in Figs. 7 and 9, the first predictions attempted by both soft-sensors are rather inaccurate. This is expected, as the number of examples presented to the networks is rather low at that point. As new information becomes available, both algorithms are adapting their parameters. The RBF algorithm builds the hidden layer by adding centers, as depicted in Fig. 8, and at the same time, adapting their synaptic weights. It can be seen that as the neural network predictors evolve themselves to adapt to the training examples, the Absolute Error for new, unknown data points is gradually reducing. After a sufficient number of training examples are presented to the networks, both soft-sensors are able to predict the ultimate compressive strength with improved accuracy. However, the superiority of the RBF sensor in terms of lower modeling error is obvious.

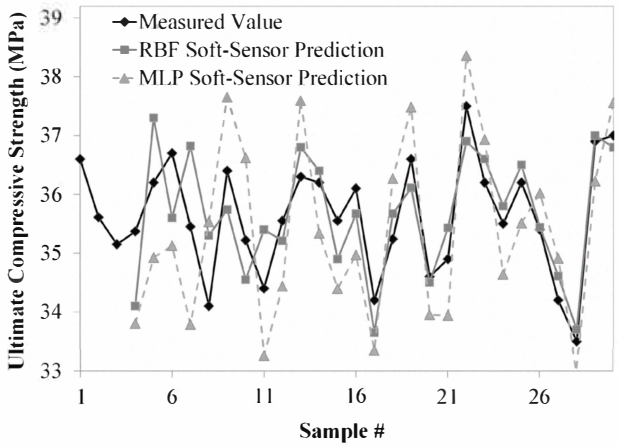

Figure 7. Measured values versus RBF and MLP soft-sensor predictions for the ultimate compressive strength

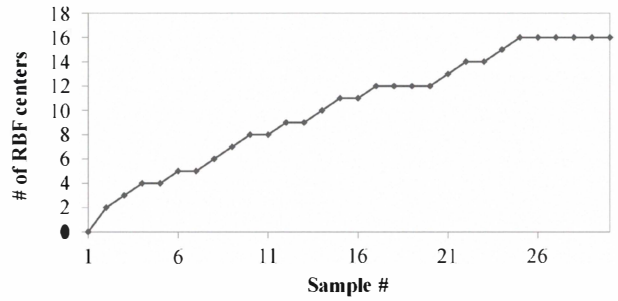

Figure 8. Evolution of the number of RBF centers in the hidden layer

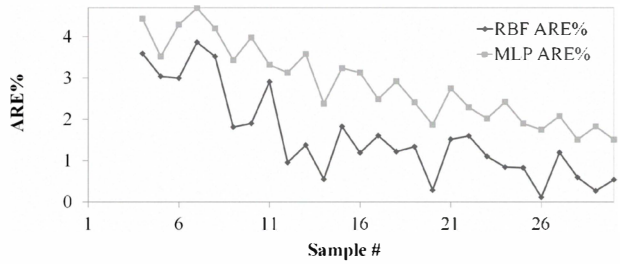

Figure 9. Evolution of the Absolute Relative Error % (ARE%) for the RBF and MLP soft-sensors

It should be noted that for this case, the forgetting factor λ and the size N_s of the moving time window were set equal to unity and infinity respectively. This actually implies that older data points were not forgotten or discarded. This choice was made, as for this particular example, the number of samples was rather small and they were presented to the soft-sensor in a random manner. Thus, it would make no sense to force the model to "forget" a portion of the recently acquired information. For longer periods, where the system could move to different operating regions (such a transition could be caused by a change in the raw materials used for making the specimens), these parameters should be tuned so that older data tend to be discarded.

V. Conclusions

In this work, we present the development of an adaptive soft-sensor able to estimate the ultimate compressive strength of cement-based materials, without having to destroy the specimen. In order to make predictions, the soft-sensor exploits the information hidden in weak electrical signals (PSCs) that are emitted when low compressive stress is applied to the specimen. The soft-sensor utilizes an RBF network initialized with zero hidden layer nodes, and based on an adaptive training technique, it manages to evolve the structure and synaptic weights of the network in order to better approximate data received online from the experimental procedure. In order to assess the efficiency of the proposed adaptive soft-sensor, experimentally measured data points were presented to it, and results have shown that it can successfully adapt itself, providing an accurate non-destructive predictor.

Acknowledgment

This research has been co-funded by the European Union (European Social Fund) and Greek national resources under the framework of the "Archimedes III: Funding of Research Groups in TEI of Athens" project of the "Education & Lifelong Learning" Operational Programme.

References

[1] P. Kadlec and B. Gabrys, "Adaptive Local Learning Soft Sensor for Inferential Control Support," in *IEEE International Conference on Computational Intelligence for Modelling Control & Automation*, Vienna, Austria, 2008, pp. 243 - 248.

[2] S. Haykin, *Neural Networks and Learning Machines*, 3rd ed. Upper Saddle River, NJ: Prentice Hall, 2009.

[3] O. Uluyol, K. Kim, and E. O. Nwadiogbu, "Synergistic Use of Soft Computing Technologies for Fault Detection in Gas Turbine Engines," *IEEE Transactions on Systems, Man, and Cybernetics - Part C: Applications and Reviews,* vol. 36, pp. 476-484, 2006.

[4] L. Fortuna, S. Graziani, and M. G. Xibilia, "Comparison of Soft-Sensor Design Methods for Industrial Plants Using Small Data Sets," *IEEE Transactions on Instrumentation and Measurement,* vol. 58, pp. 2444-2451, 2009.

[5] A. Alexandridis, D. Triantis, I. Stavrakas, and C. Stergiopoulos, "A neural network approach for compressive strength prediction in cement-based materials through the study of pressure-stimulated electrical signals," *Construction and Building Materials,* vol. 30, pp. 294–300, 2012.

[6] J. Platt, "A Resource-Allocating Network for Function Interpolation," *Neural Computation,* vol. 3, pp. 213-225, 1991.

[7] F. M. Pouzols and A. Lendasse, "Evolving fuzzy optimally pruned extreme learning machine for regression problems," *Evolving Systems,* vol. 1, p. 43, 2010.

[8] J. J. Rubio, D. M. Vazquez, and J. Pacheco, "Backpropagation to train an evolving radial basis function neural network," *Evolving Systems,* vol. 1, pp. 173–180, 2010.

[9] C.M.Bo, J.Li, S.Zhang, C.Y.Sun, and Y.R.Wang, "The Application of Neural Network Soft Sensor Technology to an Advanced Control System of Distillation Operation," in *International Joint Conference on Neural Networks*, Portland, Oregon, 2002, pp. 1054 - 1058.

[10] A. Kyriazopoulos, C. Anastasiadis, D. Triantis, and C. J. Brown, "Non-destructive evaluation of cement-based materials from pressure-stimulated electrical emission – Preliminary results," *Constr Build Mater,* vol. 25, pp. 1980-1990, 2011.

[11] C. Anastasiadis, D. Triantis, I. Stavrakas, and F. Vallianatos, "Pressure Stimulated Currents (PSC) in marble samples," *Ann Geophys,* vol. 47, pp. 21-28 2004.

[12] D. Triantis, I. Stavrakas, C. Anastasiadis, A. Kyriazopoulos, and F. Vallianatos, "An analysis of Pressure Stimulated Currents (PSC), in marble samples under mechanical stress," *Physics and Chemistry of the Earth,* vol. 31, pp. 234-239, 2006.

[13] D. Triantis, C. Anastasiadis, and I. Stavrakas, "The Correlation of Electrical Charge with Strain on Stressed Rock Samples," *Natural Hazards and Earth System Sciences,* vol. 8, pp. 1243–1248, 2008.

[14] C. Darken and J. Moody, "Fast Adaptive K-Means Clustering: Some Empirical Results," in *IEEE INNS International Joint Conference On Neural Networks*, San Diego, CA, 1990, pp. 233-238.

[15] A. Alexandridis, H. Sarimveis, G. Bafas, "A new algorithm for online structure and parameter adaptation of RBF networks," *Neural Networks,* vol. 16, pp. 1003-1017, 2003.

[16] J. Nie, "Fuzzy control of Multivariable Nonlinear Servomechanisms with Explicit Decoupling Scheme," *IEEE Transactions on Fuzzy Systems,* vol. 5, p. 304, 1997.